JOURNAL OF CATALYSIS, **99**, 391–399 (1986)

The Oxidation of Methanol on Electrolytic Silver Catalyst

BAO XINHE AND DENG JINGFA

Department of Chemistry, Fudan University, Shanghai, China

Received July 29, 1985; revised January 3, 1986

The oxidation of methanol on the surface of electrolytic silver catalyst has been investigated with Temperature-Programmed Reaction Spectroscopy (TPRS). It has been found that on a clean surface of electrolytic silver no adsorption of CH_3OH or H_2 occurred except the adsorption of small amounts of H_2O or CO_2, but the ability of silver to chemisorb the gases mentioned above was greatly enhanced by oxygen preadsorbed on the surface. In the reaction of methanol with preadsorbed oxygen-18, three distinct groups of product were observed at 400, 500 ± 20, and 620 K, respectively. At room temperature, the selective oxidation of methanol led to adsorbed surface species $CH_3O(a)$. During desorption, $CH_3O(a)$ decomposed and HCHO, $CO^{18}O$, and $H_2{}^{18}O$ were evolved simultaneously at 400 K as the first group of products. At high oxygen coverage, surface oxygen interacted with the carbon atom of $CH_3O(a)$ to form another type of stable surface intermediate $H_3CO^{18}O(a)$, which decomposed with a pseudo-second-order kinetics at 600 K, yielding only HCHO and $H_2{}^{18}O$ with a stoichiometric ratio of 2 : 1. The evolution of the second group of products CH_3OH, $CO^{18}O$, and $H_2{}^{18}O$ at 500 K was rate-limited by desorption of the products. © 1986 Academic Press, Inc.

INTRODUCTION

The oxidation of methanol to formaldehyde on a silver catalyst is one of the most important commercial processes and has been studied very intensively in the past (*1*). However, the reaction mechanism has not been clearly established. By sequentially passing streams of methanol and oxygen over a silver powder catalyst, Bhattacharyya *et al.* (*2*) clearly showed that oxygen must be present on the catalyst in order to obtain formaldehyde. Robb and Harriott (*3*) found that the reaction kinetics on a supported silver catalyst could be described by a Langmuir–Hinshelwood model in which adsorbed methanol reacted with reversibly adsorbed oxygen atoms. Wachs and Madix (*4*) examined the reaction of methanol with oxygen on a Ag(110) single crystal surface at low temperature (180 K). They observed that oxygen atoms promoted methanol adsorption and that adsorbed methanol reacted with oxygen to yield H_2O plus adsorbed methoxide species, $CH_3O(a)$. Formaldehyde was produced upon decomposition of the $CH_3O(a)$ species along with H_2 and CH_3OH; as a side product, $HCOOCH_3$ was produced.

Electrolytic silver has some excellent properties, as a commercial catalyst it can produce formaldehyde from methanol with a conversion of 98% and a selectivity of 90% (*5*). The clean surface of electrolytic silver can be easily obtained and directly used to study surface properties. The studies of surface adsorption state and surface catalysis on a commercial electrolytic silver catalyst have not been reported yet. The purpose of this paper was to investigate with TPRS the mechanism of the reaction of methanol to formaldehyde on the electrolytic silver surface and to compare the results with the previous investigation on a Ag(110) single-crystal (*4*).

EXPERIMENTAL

1. Apparatus

A refitted Ultrahigh Vacuum (UHV) system was utilized for TPRS of powder sample (*6*). The experiment chamber was equipped with a quadrupole mass spectrometer and two leak valves. Powder was

0021-9517/86 $3.00
Copyright © 1986 by Academic Press, Inc.
All rights of reproduction in any form reserved.

placed in a quartz tube directly connected to the chamber with Kovar. In order to monitor the reaction products immediately, the mouth of the quartz tube was designed to face a mass spectrometer. With a conventional electric heater and liquid-nitrogen cooler the sample can easily be heated and cooled. In the experiment, the temperature was controlled by a temperature-programming device and a good linear plot could be obtained from 1.0 to 310 K min^{-1}.

Pumping was accomplished with a cryosorption forepump and a titanium sputter ion pump (300 liters s^{-1}). The base pressure after a lower bakeout was typically 5×10^{-10} Torr. The residual gases were predominantly hydrogen and carbon monoxide. After several cycles of reaction, in addition to hydrogen and carbon monoxide, carbon dioxide and water were also observed in the residual gases, when the background pressure rose to $2\text{–}5 \times 10^{-9}$ Torr.

2. *Sample Preparation*

Silver sample is prepared by repeating the electrolysis three times, at a respective current density of 14.7 and 7 A dm^{-2}, in a 3% aquous solution of $AgNO_3$ containing 0.1% free HNO_3 at 50–55°C. The silver crystals obtained by those processes are washed free from nitrate, then dried at 120°C. Just as an industrial catalyst the particle size of the silver is about 100 μm in diameter, with a specific surface of 0.1 m^2g^{-1} and purity more than 99.999%. It was examined for surface impurities using Auger Electron Spectrometer (AES). Carbon was the only other element detected on the surface or in the near-surface region of silver. The silver sample is heated to 650°C for annealing. The resultant surface topography is shown in Fig. 1. The rough grooves and facet features are typical of electrolytic silver surface.

3. *Pretreatment and Experiment Procedures*

On a fresh silver surface no adsorption of oxygen was detected because of carbon impurities (*6, 7*). It had to be conditioned *in situ* prior to the data runs using the cleaning procedures which included high-temperature thermal etching (8×10^{-8} Torr, 920 K) and oxidation (oxygen pressure 10^{-3} Torr). Those cleaning cycles were repeated in the order given until oxygen was observed to desorb with a maximum in subsequent desorption. For electrolytic silver, more than 20 cycles were necessary so as to obtain a clean surface.

FIG. 1. Surface topography of electrolytic silver, SEM (S-520).

The dosing gases referred in the experiment are oxygen and methanol. In order to distinguish the adsorbed oxygen from that of methanol, oxygen-18 was used as a preadsorbed oxygen. The isotope ($^{18}O_2$ 99 atom%) obtained from Amersham Company can be used without further purification. Before the experiment, methanol must be processed by a complex purificatory procedure. First it was cooled with liquid nitrogen and the residual gases were pumped off by the cryosorption forepump. Then liquid nitrogen was removed and the open/close time of the pump was controlled in order to pump off the oxygen and other volatile impurities rapidly. This process was repeated several times until no impurities were detected with the exception of small amounts of water.

Typically the sample was oxidized with enriched oxygen (99% $^{18}O_2$). The mass spectrometer was always on during the adsorption process. After the desired exposure, methanol was dosed on the oxidized surface. The sample was then heated, and the various products were monitored with the mass spectrometer. In order to minimize overlap with other product signals, the methanol was monitored by recording the $m/e = 31$ signal and the other were identified by recoding the $m/e = 30(CH_2O)$, $m/e = 20(H_2{}^{18}O)$, and $m/e = 46(CO^{18}O)$ signals, etc., the results obtained were calibrated by relative strength.

RESULTS

1. Adsorption and Desorption of Oxygen on the Electrolytic Silver Surface

It was found that the sticking coefficient of oxygen on electrolytic silver is in the range of 10^{-2}–10^{-4}. The experimental results of TDS indicated that there are three distinct adsorption species on the electrolytic silver surface when oxygen exposure was less than 60 L (*6*), (see Fig. 2). Isotopic mixing and carbon monoxide titration demonstrated that the α peaks in the low-temperature range correspond to molecular chemisorbed oxygen. The β peaks were identified as chemisorbed atomic oxygen and the peaks in the high-temperature range should be ascribed to the subsurface atomic oxygen diffusion to the surface and subsequent desorption. The α state gradually disappeared with increasing oxygen exposure, when the oxygen exposure was greater than 90 L, the surface oxygen was present mainly in the dissociative atomic state. These results are consistent with those observed by XPS (VG ESCALAB-5) (*8*). The oxygen coverage of electrolytic silver varies with exposure as shown in Fig. 3.

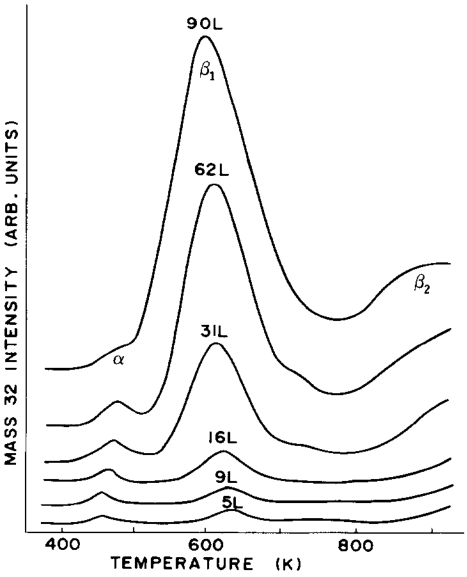

FIG. 2. Thermal desorption spectra for adsorbed oxygen on silver at 295 K, heating rate 0.5 K s^{-1}.

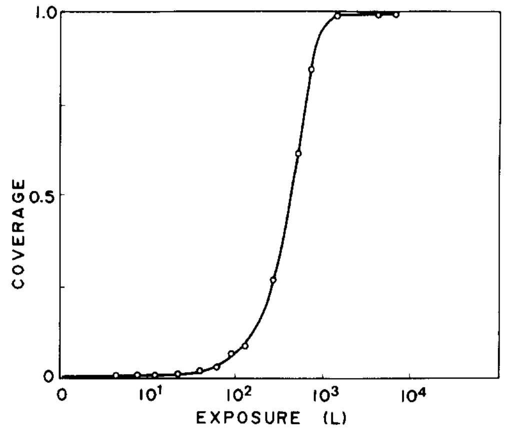

FIG. 3. Coverage vs exposure profiles for oxygen on silver at 295 K.

2. CH_3OH, H_2, CO_2, and H_2O Adsorption and Desorption on Electrolytic Silver Surface

Experiments show that no adsorption of CH_3OH or H_2 occurred on the clean electrolytic silver surface but for small amounts of H_2O and CO_2, however, the ability of silver to chemisorb all of the gases above was greatly enhanced by surface preadsorbed oxygen. Figure 4 shows the effect of the coverage of surface oxygen species upon the amounts of adsorbed H_2, CO_2, and H_2O in a given range of preadsorbed oxy-

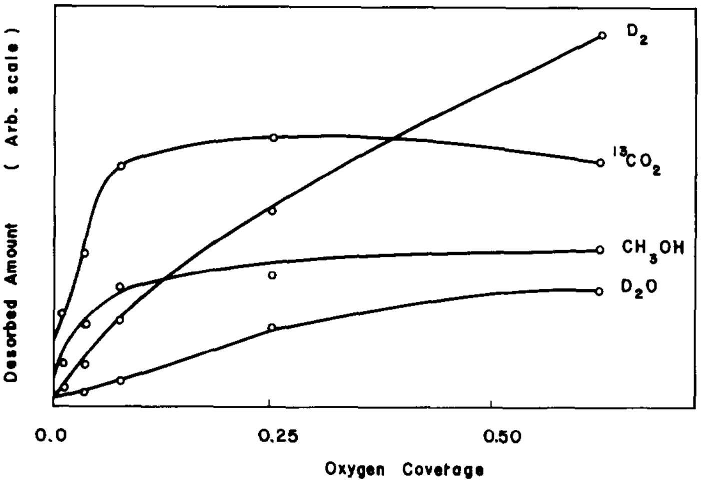

FIG. 4. The influence of oxygen coverage upon the amounts of adsorbed D_2, $^{13}CO_2$, D_2O, and CH_3OH.

gen coverage and Table 1 shows the desorption parameters of various gases on the silver surface with preadsorbed oxygen. The detailed result that H_2, CO_2, and H_2O interact with preadsorbed oxygen on the electrolytic silver surface will be published elsewhere.

3. *Reaction of Methanol with Preadsorbed Oxygen*

The purified methanol was dosed onto a silver surface with a given oxygen coverage (exposure). After reaching the desired exposure, the variable leak valve was turned off and the residual methanol in the gas phase was rapidly pumped off. The signals of reaction products were simultaneously recorded at a given *m/e* with the mass spectrometer during the programmed heating. Figures 5a, b, and c show the product distribution obtained from the reaction of methanol with preadsorbed oxygen at 0.03, 0.08, and 0.50 of coverage, respectively. It can be seen from the curves in Figs. 5b and c that there are three distinct groups of products at 400 ± 3, 500 ± 20, and 620 ± 2 K, respectively, with increasing sample temperature. These results reveal that the methanol reacts with the ^{18}O atoms on the electrolytic silver surface to produce HCHO, $H_2{}^{18}O$, and $CO^{18}O$ as products. The desorption kinetic parameters for all the products are listed in Table 2.

By comparing the results in Table 2 with those in Table 1, we can see that the kinetic parameters for second group of products (CH_3OH, H_2CO,$CO^{18}O$, and $H_2{}^{18}O$) obtained in the oxidation of methanol are identical to those obtained in the desorption of these gases themselves. The results indicate that those products are from desorption step and not from formation process. In other words, the rate-limiting step for the evolution of the second group is the desorption of these species (*10*). In contrast with

TABLE 1

Characteristic Desorption Parameters for Several Molecules Species Monitored from the Electrolytic Silver Surface with Preadsobed Oxygen Coverage 0.08

Molecule	T_p (K)	E_d (kcal/mol)
D_2/D_2	476	22.9
$^{13}CO_2/^{13}CO_2$	475	16.0
$D_2O/D_2O(\alpha_1)$	410 ± 5	9.2[a]
$D_2O/D_2O(\alpha_2)$	456 ± 5	12.0[a]

[a] The activation energies, E_d, were calculated by plotting ln P versus $1/T_p$ (*9*) and the other by the method of peak width analysis. The data in Table 2 were obtained in the same way.

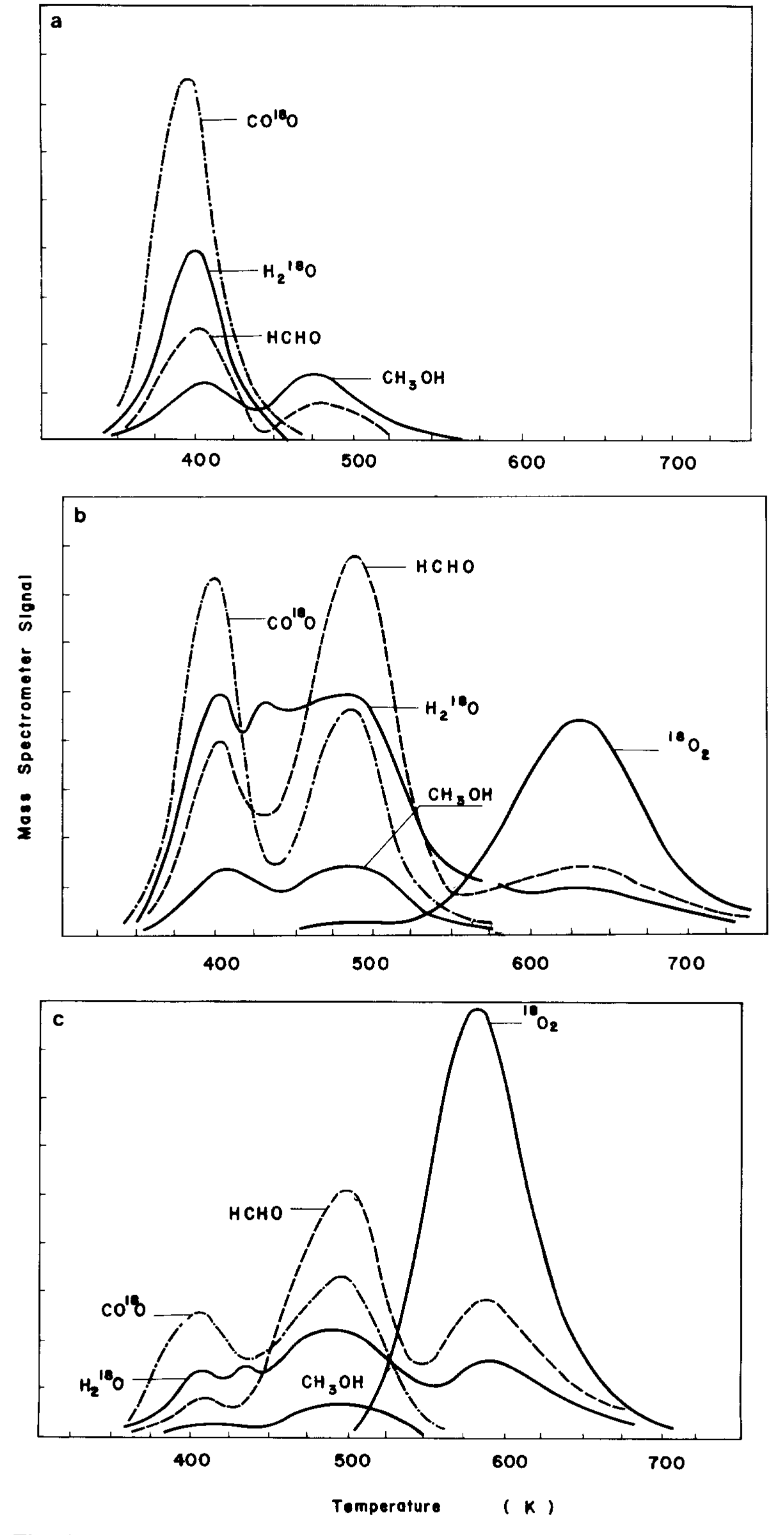

FIG. 5. The thermal programmed reaction spectra obtained following CH_3OH adsorption on an electrolytic silver surface on which oxygen-18 was preadsorbed at 297 K. The CH_3OH exposures were always 144 L; the $^{18}O_2$ coverages were (a) 0.03, (b) 0.08, and (c) 0.50.

TABLE 2

The Kinetic Parameters Observed for Oxidation of CH_3OH on the Electrolytic Silver Surface

First group of products			Second group of products			Third group of products		
Product	T_p(K)	E_d (kcal/mol)	Product	T_p(K)	E_d (kcal/mol)	Product	T_p(K)	E_d (kcal/mol)
CH_3OH	401	21.5	CH_3OH	492	—	HCHO	635	22.3
HCHO	398	24.1	HCHO	489	18.1	$H_2{}^{18}O$	635	23.5
$CO^{18}O$	397	24.0	$CO^{18}O$	478	16.6	$^{18}O_2$	628	31.3
$H_2{}^{18}O$	398	23.1	$H_2{}^{18}O(\alpha_1)$	415 ± 3	—			
			$H_2{}^{18}O(\alpha_2)$	458 ± 3	12.9[a]			

Note. The preadsorbed oxygen coverage was 0.08 and exposure of CH_3OH was 144 L at 297 K. The heating rate was 64 K/min.

[a] See footnote of Table 1.

this, there are obvious distinctions in the kinetic parameters between the other two groups and those of pure substances. According to this it suggests that the evolution of both first and third groups of products are different from the desorption of pure substance and must be rate-limited for its formation.

The data of Table 2 show that the kinetic parameters of the first group of products (HCHO, CH_3OH,$CO^{18}O$, and $H_2{}^{18}O$) are very close, i.e., T_p was found to be within 399.0 ± 2 K and E_d within 23 ± 1 kcal/mol for all of the species. The observed peak shapes of the products were also similar (Fig. 5). Similarly, for the two products (HCHO, and $H_2{}^{18}O$) in the third group, T_p, E_d, and the peak shape were almost identical. Based on the principle of TPRS (*10*), reaction products having the same peak shape and temperature originate from the same rate-limiting step; in addition, the energetic quantity being measured is the activation energy for the surface reaction, not a binding energy. Thus the above results are strong evidence that the species appearing in each of two groups are formed simultaneously in a single surface reaction-limited step, and the first group and the third group correspond to different surface reactions.

The amount of products in the third group varies with the coverage of preadsorbed oxygen as shown in Fig. 6. By comparing Fig. 6 with Fig. 5, we can see that for the first group the peak temperatures (T_p) did not vary with the coverage of preadsorbed oxygen but the T_p of the third group ($H_2{}^{18}O$ and HCHO) shifted to lower temperature with increasing preadsobed oxygen coverage. This result indicates that for the first group of products the rate-limiting step corresponds to first-order kinetics, whereas the kinetics of the third group of products may be explained with a second-order surface reaction. Plotting the evolved amounts of product $H_2{}^{18}O$ versus HCHO for the third group of products in Fig. 7 yields a straight line with a slope of about 2. This result provides direct information on the atomic composition of the rate-determining active intermediate.

4. *Effect of Preadsorbed Oxygen upon Product Distribution*

The amounts of main products (HCHO and $CO^{18}O$) from the oxidation of methanol vary with the coverage of preadsorbed oxygen as presented in Fig. 8. It shows that at lower oxygen coverages the amounts of products were very small, whereas they rapidly increased with increasing coverage. The HCHO amount reached its maximum at $\theta = 0.25$; further increases in oxygen coverage enhanced the amount of the by-product $CO^{18}O$.

The studies (*5*, *11*) of catalytic activity for the oxidation of methanol to formaldehyde on the electrolytic silver show that methanol conversion, formaldehyde yield, and the amount of carbon dioxide are small at lower ratios of oxygen to methanol, *n*(oxygen)/*n*(methanol). With an increase of the ratio, formaldehyde yield and the amount of CO_2 are gradually enhanced. Further increases in the ratio promotes CO_2 formation and reduces the selectivity for H_2CO. These results are in accord with those obtained in this paper.

DISCUSSION

Wachs and Madix (*4*) reported their results concerning the reaction mechanism of methanol oxidation on a Ag(110) single-crystal with preadsorbed oxygen. They pointed out that due to interaction with preadsorbed oxygen the methanol is dissociatively adsorbed and then forms adsorbed methoxide ($CH_3O(a)$). During the flash, the methoxide species decompose via dehydrogenation with the help of oxygen to HCHO, CO_2, etc. Adsorbed $CH_3O(a)$ also reacts with HCHO to form H_2COOCH_3 which subsequently yields $HCOOCH_3$ and H_2. The different reaction pathways available to surface methoxide $CH_3O(a)$ on Ag(110) are schematically presented as follows:

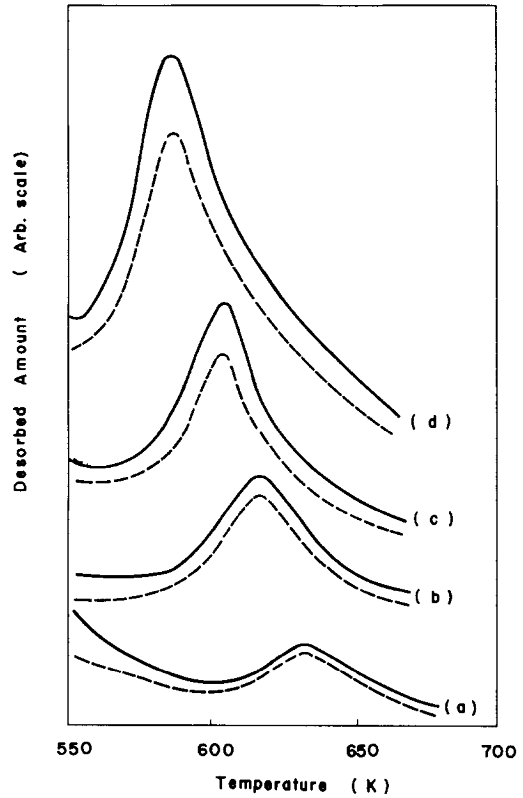

FIG. 6. The influence of oxygen coverage upon the amounts of desorbed HCHO and $H_2{}^{18}O$ in the third group of products. Oxygen coverages: (a) 0.20, (b) 0.5, (c) 0.65, (d) 0.80. (—) HCHO; (---) $H_2{}^{18}O$.

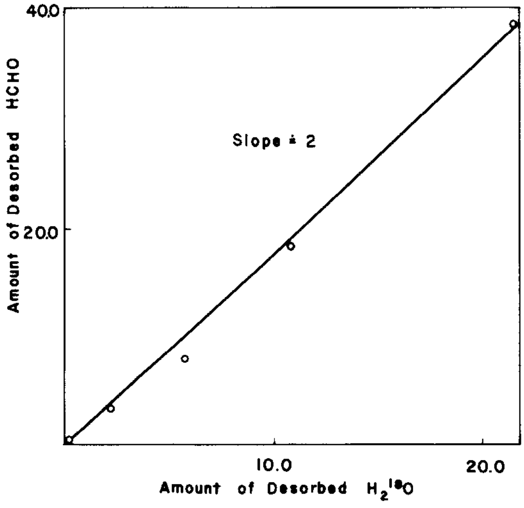

FIG. 7. The relation of the evolution of HCHO and $H_2{}^{18}O$ for the third group of products.

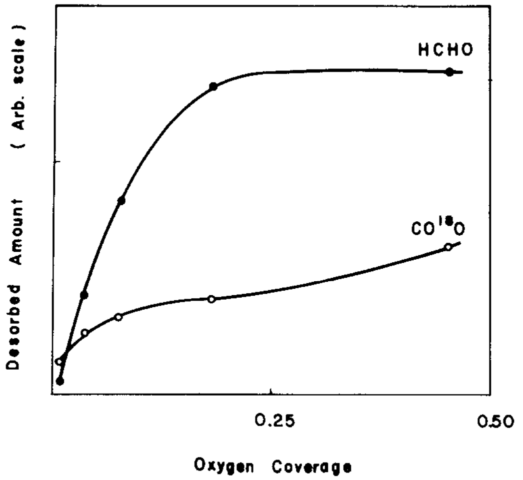

FIG. 8. The influence of oxygen coverage upon the amounts of evolution of HCHO and $CO^{18}O$. The exposure of CH_3OH was 144 L.

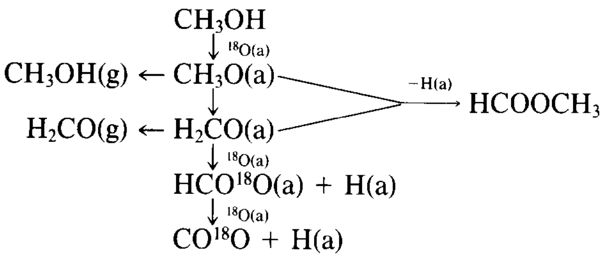

Owing to the physical characteristic and surface structure mentioned above the results obtained on the electrolytic silver differ from those obtained on clean Ag(110) single-crystal in three important aspects. First, methanol reaction with preadsorbed oxygen on electrolytic silver results in three groups of products appearing over different temperature regions. The product spectra revealed that for the first and third groups the rate-controlling step is surface reaction, whereas the evolution of products in the second group is rate-limited by desorption of the product gases. Second, no methylformate was observed in all of the three groups of products. This agrees with the results of activity measurements by the flowing method (*11*). Third, the various products formed on a Ag(110) single-crystal result from the further oxidation of the adsorbed methoxide intermediate, but on the electrolytic silver surface with high oxygen coverage another type of stable surface intermediate, different from methoxide is present. The third group of products results from its decomposition.

Based on the experimental results, the first group of products is obtained by the following reaction steps:

$$CH_3OH(g) + {}^{18}O(a) \rightarrow CH_3O(a) + H^{18}O(a) \quad (1)$$

$$CH_3O(a) + {}^{18}O(a) \rightarrow H_2CO(a) + H^{18}O(a) \quad (2)$$

$$CH_3O(a) + CH_3OH^{\oplus 18}O(a) \rightarrow CH_3O(a) + CH_3OH(g) + {}^{18}O(a) \quad (3)$$

$$H_2CO(a) \rightarrow H_2CO(g) \quad (4)$$

$$H_2CO(a) + {}^{18}O(a) \rightarrow H_2CO^{18}O(a) \quad (5)$$

$$H_2CO^{18}O(a) + {}^{18}O \rightarrow HCO^{18}O(a) + H^{18}O(a) \quad (6)$$

$$HCO^{18}O(a) + {}^{18}O(a) \rightarrow CO^{18}O(a) + H^{18}O(a) \quad (7)$$

$$CO^{18}O(a) \rightarrow CO^{18}O(g) \quad (8)$$

$$H^{18}O(a) + H^{18}O(a) \rightarrow H_2{}^{18}O(a) + {}^{18}O(a) \quad (9)$$

$$H_2{}^{18}O(a) \rightarrow H_2{}^{18}O(g) \quad (10)$$

The symbol ⊕ (Eq. (3)) indicates the induced adsorption of the alcohol by the preadsorbed oxygen.

From the above reaction mechanism, the first group of products should comprise H_2CO, $CO^{18}O$, CH_3OH, and $H_2{}^{18}O$ which agrees with the experimental results. The peak shape temperature of product evolution and the kinetic parameters of the above, which can be seen in Fig. 5 and Table 2, are similar. This indicates that they originate from a common adsorbed $CH_3O(a)$ intermediate and share a same rate-limiting step of surface reaction.

At low coverage of oxygen, surface oxygen interacts quantitively with methanol without remains of oxygen on the surface. Owing to the very small sticking coefficient and low desorption activation energy of product molecules on clean electrolytic silver, the reaction products immediately leave the surface for the gas phase, as shown in Fig. 5a. As the coverage of preadsorbed oxygen increases, some adsorbed oxygen which is not used up remains on the surface. Due to the inducing adsorption effect of adsorbed oxygen, part of the products in the above-mentioned reactions interact strongly with surface oxygen and remain on the surface as follows:

$$H_2{}^{18}O(a) + {}^{18}O(a) \rightarrow H^{18}O(a) + H^{18}O(a) \tag{11}$$

$$CO^{18}O + {}^{18}O(a) \rightarrow {}^{18}OCO^{18}O(a) \tag{12}$$

$$H_2CO(a) + {}^{18}O(a) \rightarrow H_2CO^{\oplus 18}O(a) \tag{13}$$

$$CH_3OH + {}^{18}O(a) \rightarrow CH_3OH^{\oplus 18}O(a) \tag{14}$$

As the characteristic desorption temperature is reached, the adsorbed species in (11)–(14) immediately desorb from the surface:

$$H^{18}O(a) + H^{18}O(a) \rightarrow H_2{}^{18}O(g) + {}^{18}O(a) \tag{15}$$

$${}^{18}OCO^{18}O(a) \rightarrow CO^{18}O(g) + {}^{18}O(a) \tag{16}$$

$${}^{18}OCO^{18}O(a) \rightarrow {}^{18}OC^{18}O(g) + O(a) \tag{17}$$

$$H_2CO^{\oplus 18}O(a) \rightarrow H_2CO(g) + {}^{18}O(a) \tag{18}$$

$$CH_3OH^{\oplus 18}O(a) \rightarrow CH_3OH(g) + {}^{18}O(a) \tag{19}$$

At high remaining oxygen coverage, the adsorbed atomic oxygen around the methoxide attacks to the carbon atom in the surface methoxide species to form a stable intermediate as shown in the scheme

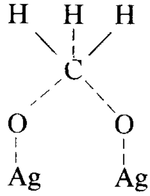

It can be seen from Table 2 that $^{18}O_2$ desorption peaks at 628 K—slightly below the temperature at which the maximum in H_2CO and $H_2{}^{18}O$ desorption occurs. This suggests that O(a) can stabilize the H_3CO $^{18}O(a)$ intermediate and decomposition only occurs after oxygen desorbs from the vicinity of an $H_3CO^{18}O$ species. Thus $H_3CO^{18}O$ decomposition, which leads to the third group of products, would show pseudo-second-order kinetics which mimic those of O_2 desorption. The mechanism is formulated as follows:

$$H_3CO^{18}O(a) \rightarrow H_2CO(a) + H^{18}O(a) \tag{20}$$

$$H_2CO(a) \rightarrow H_2CO(g) \tag{21}$$

$$H^{18}O(a) + H^{18}O(a) \rightarrow H_2{}^{18}O(g) + {}^{18}O(a) \tag{22}$$

Where, step (20) is a rate-limiting process. Owing to the fact that the reactions occur at high temperature, formaldehyde formed in step (21) immediately desorbs from the surface and which prevented from further oxidation. According to this mechanism it should yield only formaldehyde and water, and the ratio of formaldehyde to water should be 2 : 1. This is in accord with the experimental result in Fig. 7.

REFERENCES

1. Bartern, M. A., and Madix, R. J., "Chemical Physics of Solid Surface and Heterogeneous Catalysis," Vol. 4, p. 139. Elsevier, Amsterdam, 1982.
2. Bhattacharyya, S. K., Nag, N. K., and Ganguly, N. D., *J. Catal.* **23,** 158 (1971).
3. Robb, D. A., and Harriott, P., *J. Catal.* **35,** 176 (1974).
4. Wachs, I. E., and Madix, R. J., *Surf. Sci.* **76,** 531 (1978).
5. Deng, J. F., Xiang, Y. F., Ji, X. H., and Chong, X. Z., *Petrochem. Technol. (China)* **9,** 523 (1980).
6. Deng, J. F., Bao, X. H., and Guo, B. L., *Acta Phys.-Chim. Sin. (China).* **1,** 39 (1985).
7. Ekern, R. J., and Czanderna, A. W., *J. Catal.* **46,** 109 (1977).
8. Bao, X. H., Deng, J. F., and Dong, S. Z., *Surf. Sci.* **163,** 444 (1985).
9. Habenschaden, E., and Kuppers, J., *Surf. Sci.* **138,** L147 (1984).
10. Madix, R. J., *CRC Crit. Rev. Solid State Mater. Sci.* **7,** 143 (1978).
11. Deng, J. F., Xiang, Y. F., Ye, L. Y., and Zhu, X. Z., *J. Catal. (Dalian)* **4,** 266 (1983).